

## Acid-Catalyzed Photoreduction of Dialkyl Sulfoxides by an Acid-Stable NADH Analogue

Shunichi Fukuzumi\* and Yoshihiro Tokuda

Department of Applied Chemistry, Faculty of Engineering, Osaka University, Suita, Osaka 565, Japan

Received: August 7, 1992; In Final Form: January 19, 1993

Photoreduction of dialkyl sulfoxides ( $R_2SO$ ) by an acid-stable NADH analogue, 10-methyl-9,10-dihydroacridine ( $AcrH_2$ ), proceeds in the presence of perchloric acid in acetonitrile containing  $H_2O$  (0.50 M) to yield 10-methylacridinium ion ( $AcrH^+$ ) and the corresponding dialkyl sulfides ( $R_2S$ ). No photoreduction of  $R_2SO$  by  $AcrH_2$  has occurred in the absence of perchloric acid. In the presence of perchloric acid the protonation of dialkyl sulfoxides occurs to increase the oxidizing ability of the sulfoxides significantly, when the singlet excited state ( $^1AcrH_2^*$ ) is quenched efficiently by the protonated sulfoxides ( $R_2SOH^+$ ). The  $^1AcrH_2^*$  is also quenched by  $HClO_4$ . The dependence of quantum yields on  $[R_2SOH^+]$  indicates that the photoreduction of  $R_2SO$  by  $AcrH_2$  proceeds via electron transfer from  $^1AcrH_2^*$  to  $R_2SOH^+$ , followed by the hydrogen transfer from  $AcrH_2^{*+}$  to  $R_2SOH^+$ , accompanied by the concomitant dehydration to yield  $AcrH^+$  and  $R_2S$ .

## Introduction

The use of the excited states of NADH analogues has been shown to be effective for the reduction of various substrates by NADH analogues.<sup>1-3</sup> A number of substrates can also be reduced readily by acid-stable NADH analogues such as 10-methyl-9,10-dihydroacridine ( $AcrH_2$ ) in the presence of  $HClO_4$  in acetonitrile ( $MeCN$ ).<sup>3,4</sup> However, neither thermal acid catalysis nor the use of the excited states of NADH analogues has been effective for the reduction of dimethyl sulfoxide ( $Me_2SO$ ), which is commonly used as an inert aprotic solvent. In the biological system, the pathway of  $Me_2SO$  metabolism is known to involve the initial reduction of  $Me_2SO$  to dimethyl sulfide ( $Me_2S$ ) by NADH being an electron donor.<sup>5</sup> On the other hand, there has been considerable interest in acid-catalyzed photochemical reactions in which the use of excited states and acid catalysis are combined to achieve high efficiencies for the reactions of interest.<sup>6-8</sup> However, few examples have so far been reported with regard to acid-catalyzed photoredox reactions.<sup>9</sup>

In this study we report that the use of the excited state of  $AcrH_2$  combined with acid catalysis makes it possible for the first time to reduce  $Me_2SO$  and other dialkyl sulfoxides by an acid-stable NADH analogue, 10-methyl-9,10-dihydroacridine ( $AcrH_2$ ) in the presence of perchloric acid ( $HClO_4$ ) in  $MeCN$  to yield 10-methylacridinium ion ( $AcrH^+$ ) and the corresponding dialkyl sulfides ( $R_2S$ ).<sup>10</sup> The use of an acid-stable NADH analogue is essential to examine the acid-catalyzed reactions, since ordinary NADH analogues are known to decompose in the presence of acids.<sup>11</sup> The reaction mechanism of the acid-catalyzed photoreduction of  $R_2SO$  by  $AcrH_2$  is revealed based on determination of the protonation equilibrium of  $R_2SO$ , the dependence of the quantum yields on the concentrations of  $R_2SO$  and  $HClO_4$ , and the fluorescence quenching of  $AcrH_2$  by  $R_2SO$  as well as the lifetime measurements in the presence of  $HClO_4$ .

## Experimental Section

**Materials.** 10-Methyl-9,10-dihydroacridine ( $AcrH_2$ ) was prepared from 10-methylacridinium iodide ( $AcrH^+I^-$ ) by the reduction with  $NaBH_4$  in methanol and purified by recrystallization from ethanol.<sup>12</sup> 10-Methylacridinium iodide was prepared by the reaction of acridine with methyl iodide in acetone and it was converted to the perchlorate salt ( $AcrH^+ClO_4^-$ ) by the addition of magnesium perchlorate to the iodide salt and purified by recrystallization from methanol.<sup>13</sup> The deuterated compound,  $[9,9\text{-}^2H_2]$ -10-methylacridine ( $AcrD_2$ ) was prepared from

10-methylacridone by the reduction with  $LiAlD_4$ .<sup>14</sup> Dialkyl sulfoxides and dialkyl sulfides were obtained commercially. For safety reasons  $HClO_4$  (70%) containing 30% water was used in this study. Acetonitrile used as a solvent was purified and dried by the standard procedure.<sup>15</sup>

**Analytical Procedure.** Typically,  $AcrH_2$  ( $3.6 \times 10^{-5}$  mol) was added to an NMR tube which contained deaerated  $[^2H_3]$ acetonitrile ( $CD_3CN$ ) solution (0.60 cm<sup>3</sup>) of  $R_2SO$  (0.10 M),  $HClO_4$  (0.20 M), and  $H_2O$  (0.50 M) under an atmospheric pressure of argon. The reactant solution was then irradiated with light from a Ushio Model UI-501C xenon lamp for 20 h. The products were identified as 10-methylacridinium ion ( $AcrH^+$ ) and  $R_2S$  by the  $^1H$  NMR spectra by comparing with those of the authentic samples. The  $^1H$  NMR measurements were performed using Japan Electron Optics JNM-PS-100 (100 MHz) and JNM-GSX-400 (400 MHz) NMR spectrometers.  $^1H$  NMR ( $CD_3CN$ ):  $AcrH^+ClO_4^-$   $\delta$  4.76 (s, 3H), 7.9-8.8 (m, 8H), 9.87 (s, 1H). The yields of  $R_2S$  were also determined by using a Shimadzu GC-7A gas-liquid chromatograph equipped with a SE-30 column.

The protonation equilibrium constants ( $K$ ) of  $R_2SO$  were determined from the change in the absorbance ( $\Delta A/\Delta A_0$ ) at  $\lambda = 220$  nm due to the protonation of  $R_2SO$  as given by eq 1, where  $[R_2SO]_0$  and  $[H^+]_0$  are the initial concentrations of  $R_2SO$  and  $HClO_4$ , respectively. The best fit values were obtained by the computer simulation; the experimental errors are  $\leq \pm 10\%$ .

$$\Delta A/\Delta A_0 = (2[R_2SO]_0)^{-1}([R_2SO]_0 - [H^+]_0 - K^{-1} + \{([R_2SO]_0 + [H^+]_0 + K^{-1})^2 + 4[H^+]_0[R_2SO]_0\}^{1/2}) \quad (1)$$

**Quantum Yield Determinations.** A standard actinometer (potassium ferrioxalate)<sup>16</sup> was used for the quantum yield determination of the acid-catalyzed photoreduction of  $R_2SO$  by  $AcrH_2$ . A square quartz cuvette (10 mm i.d.) which contained an  $MeCN$  solution (2.0 cm<sup>3</sup>) of  $AcrH_2$  ( $2.0 \times 10^{-3}$  M),  $HClO_4$  ( $5.0 \times 10^{-3}$  to  $1.0 \times 10^{-1}$  M), and  $H_2O$  (0.50 M) was irradiated with monochromatized light of  $\lambda = 320$  nm from a Hitachi 650-10S fluorescence spectrophotometer. Under the conditions of actinometry experiments, both the actinometer and  $AcrH_2$  absorbed essentially all the incident light of  $\lambda = 320$  nm. The light intensity of monochromatized light of  $\lambda = 320$  nm was determined as  $1.12 \times 10^{-6}$  einstein  $dm^{-3} s^{-1}$  with the slit width of 10 nm. The photochemical reaction was monitored using a Union SM-401 spectrophotometer. The quantum yields were

determined from the increase in absorbance due to AcrH<sup>+</sup> ( $\lambda_{\max}$  = 358 nm,  $\epsilon_{\max}$  =  $1.8 \times 10^4$  M<sup>-1</sup> cm<sup>-1</sup>).

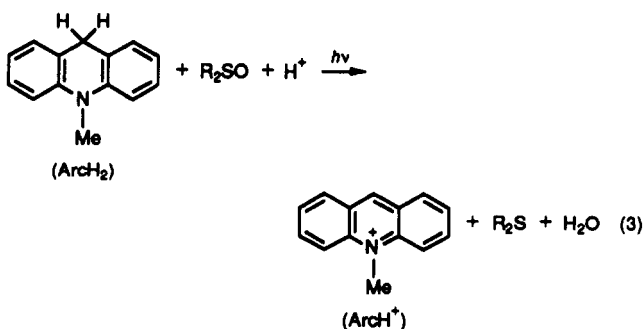
**Fluorescence Measurements.** Fluorescence measurements were carried out on a Shimadzu RF-5000 spectrofluorophotometer. The fluorescence spectra of AcrH<sub>2</sub> were measured in the presence of various concentrations of HClO<sub>4</sub> in MeCN containing H<sub>2</sub>O (0.50 M) at 298 K. Fluorescence lifetimes were measured using a Horiba NAES-1100 time-resolved spectrofluorophotometer. In the quenching experiments, the excitation wavelength of AcrH<sub>2</sub> was 320 nm, which excites AcrH<sub>2</sub> selectively. Relative fluorescence lifetimes were measured for MeCN solution containing AcrH<sub>2</sub> ( $5.0 \times 10^{-5}$  M), H<sub>2</sub>O (0.50 M), and various concentrations of HClO<sub>4</sub> ( $1.0 \times 10^{-3}$  to  $1.0 \times 10^{-2}$  M). The Stern–Volmer relation (eq 2) was obtained between the ratio of the lifetime in the absence and presence of HClO<sub>4</sub> ( $\tau_0/\tau$ ) and [HClO<sub>4</sub>].

$$\tau_0/\tau = 1 + k_q \tau_0 [\text{HClO}_4] \quad (2)$$

**Theoretical Calculations.** Theoretical studies were performed using the PM3 molecular orbital method.<sup>17,18</sup> The MOPAC program (QCPE No. 455), which was revised as OS/2 Version 5.01 to adapt for the use on a NEC PC computer was obtained through the Japan Chemistry Program Exchange (JCPE).<sup>19</sup> The calculations were also performed by using the MOL-GRAFF program, version 2.8, by Daikin Industries, Ltd. The structural output was recorded by using the MOPC program (JCPE No. P038). Final geometry and energetics were obtained by optimizing the total molecular energy with respect to all structural variables. The geometry of the radical cation (AcrH<sub>2</sub><sup>•+</sup>) was optimized using the unrestricted Hartree–Fock (UHF) formalism. The value of heat of formation ( $\Delta H_f$ ) of AcrH<sub>2</sub><sup>•+</sup> was calculated with the UHF-optimized structures using the half-electron (HE) method with the restricted Hartree–Fock (RHF) formalism.<sup>20</sup> The  $\Delta H_f$  values of Me<sub>2</sub>SO<sup>•-</sup> and Me<sub>2</sub>SOH<sup>•</sup> were calculated with the RHF-optimized structures. The  $\Delta H_f$  value of the singlet excited state (<sup>1</sup>AcrH<sub>2</sub><sup>\*</sup>) was calculated with the key word “EXCITED” by optimizing the total molecular energy with respect to all structural variables.

## Results and Discussion

**Photoreduction of Dialkyl Sulfoxides by AcrH<sub>2</sub>.** The AcrH<sub>2</sub> shows no reactivity toward Me<sub>2</sub>SO in the presence of HClO<sub>4</sub> in MeCN in the dark. No photoreduction of Me<sub>2</sub>SO by AcrH<sub>2</sub> has occurred in the absence of HClO<sub>4</sub> in MeCN, either. When HClO<sub>4</sub> and photoirradiation are combined together, however, Me<sub>2</sub>SO can be reduced efficiently by AcrH<sub>2</sub> to yield 10-methylacridinium ion (AcrH<sup>+</sup>) and dimethyl sulfide as shown in eq 3 (see Experimental Section). Other dialkyl sulfoxides [Bu<sub>2</sub>SO,



(PhCH<sub>2</sub>)<sub>2</sub>SO] are also reduced by AcrH<sub>2</sub> in the presence of HClO<sub>4</sub> in MeCN under photoirradiation as shown in Table I. In the presence of HClO<sub>4</sub> (70%, 0.20 M) both AcrH<sub>2</sub> and R<sub>2</sub>SO are readily protonated in MeCN judging from the change in their electronic absorption and <sup>1</sup>H NMR spectra in the presence of HClO<sub>4</sub>.<sup>21,22</sup> When H<sub>2</sub>O (0.50 M) is added to the MeCN solution, however, only R<sub>2</sub>SO is protonated (eq 4) while essentially no

**TABLE I: Photoreduction of Dialkyl Sulfoxides (0.10 M) by AcrH<sub>2</sub> ( $5.7 \times 10^{-2}$  M) in the Presence of HClO<sub>4</sub> and H<sub>2</sub>O (0.50 M) in MeCN at 298 K under Irradiation with a Xenon Lamp**

substrate	[HClO <sub>4</sub> ]/M	product (yield/%) <sup>a</sup>
Me <sub>2</sub> SO	0	No reaction
Me <sub>2</sub> SO	0.20	AcrH <sup>+</sup> (90) Me <sub>2</sub> S (87)
Bu <sub>2</sub> SO	0	No reaction
Bu <sub>2</sub> SO	0.20	AcrH <sup>+</sup> (92) Bu <sub>2</sub> S (92)
(PhCH <sub>2</sub> ) <sub>2</sub> SO	0	No reaction
(PhCH <sub>2</sub> ) <sub>2</sub> SO	0.20	AcrH <sup>+</sup> (92) (PhCH <sub>2</sub> ) <sub>2</sub> S (92)

<sup>a</sup> Irradiation time: 20 h.

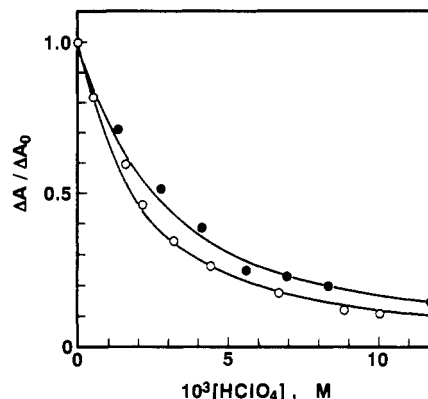


**Figure 1.** Change in absorbance at  $\lambda = 220$  nm due to the protonation of Me<sub>2</sub>SO (O) and Bu<sub>2</sub>SO (●) with an increase in [HClO<sub>4</sub>] in MeCN containing H<sub>2</sub>O (0.50 M) at 298 K. The solid lines are drawn with  $K = 8.0 \times 10^2$  and  $5.0 \times 10^2$  M<sup>-1</sup> for the protonation of Me<sub>2</sub>SO and Bu<sub>2</sub>SO by using eq 1, respectively.

protonation of AcrH<sub>2</sub> takes place. Figure 1 shows the change in



the absorbance due to R<sub>2</sub>SO ( $\lambda = 220$  nm, R = Me and Bu) in the presence of HClO<sub>4</sub> in MeCN containing H<sub>2</sub>O (0.50 M). The protonation equilibrium constants ( $K$ ) are obtained by computer simulation based on eq 1 as  $8.0 \times 10^2$  and  $5.0 \times 10^3$  M<sup>-1</sup> for Me<sub>2</sub>SO and Bu<sub>2</sub>SO, respectively (see Experimental Section). The solid lines in Figure 1 are drawn by using the  $K$  values based on eq 1, demonstrating good agreement with the experimental values.<sup>23</sup> The protonation of R<sub>2</sub>SO may enhance the oxidizing ability significantly as reported for the case of flavin analogues.<sup>3,24</sup>

The quantum yields ( $\Phi$ ) of the photoreduction of R<sub>2</sub>SO by AcrH<sub>2</sub> and the 9,9'-dideuterated compound (AcrD<sub>2</sub>) in the presence of HClO<sub>4</sub> in MeCN containing H<sub>2</sub>O (0.50 M) were determined by using an iron(III) oxalate actinometer (see Experimental Section).<sup>16</sup> The increase in the H<sub>2</sub>O concentration from 0.50 to 2.0 M in the presence of HClO<sub>4</sub> (0.10 M) resulted in little effect on the  $\Phi$  value (0.045 at [H<sub>2</sub>O] = 0.50 M, 0.043 at [H<sub>2</sub>O] = 2.0 M). The  $\Phi$  value increases with an increase in the HClO<sub>4</sub> concentration to reach a maximum value and then decreases in the high HClO<sub>4</sub> concentrations as shown in Figure 2. The increase in the  $\Phi$  value corresponds to the increase in [Me<sub>2</sub>SOH<sup>+</sup>] which reaches a constant value when all Me<sub>2</sub>SO molecules are protonated. It should be noted that no primary kinetic isotope effect is observed when AcrH<sub>2</sub> is replaced by AcrD<sub>2</sub>;  $\Phi_{\text{H}}/\Phi_{\text{D}} = 1.0 \pm 0.1$  (Figure 2). The retarding effect of HClO<sub>4</sub> in high [HClO<sub>4</sub>] in Figure 2 may be ascribed to the quenching of <sup>1</sup>AcrH<sub>2</sub><sup>\*</sup> by the protonation with HClO<sub>4</sub> (eq 5). In fact, the



fluorescence lifetime of AcrH<sub>2</sub> ( $5.0 \times 10^{-5}$  M) in MeCN containing H<sub>2</sub>O (0.50 M) is reduced by addition of HClO<sub>4</sub> as

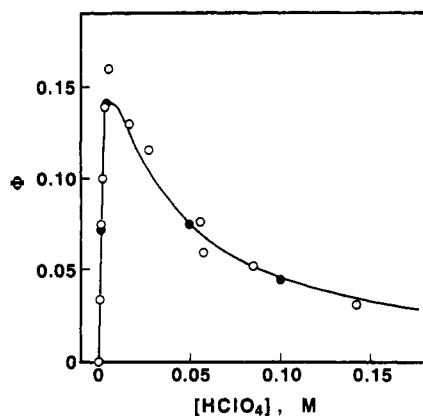


**Figure 2.** Dependence of the quantum yield  $\Phi$  on  $[\text{HClO}_4]$  for the photoreduction of  $\text{Me}_2\text{SO}$  ( $3.4 \times 10^{-3}$  M) by  $\text{AcrH}_2$  (O) and  $\text{AcrD}_2$  (●) in the presence of  $\text{HClO}_4$  and  $\text{H}_2\text{O}$  (0.50 M) in MeCN at 298 K. The solid line is drawn with the rate constants ( $k_{et}$  and  $k_H$ ), the fluorescence lifetime ( $\tau_0$ ), and the protonation equilibrium constant ( $K$ ) by using eq 10.

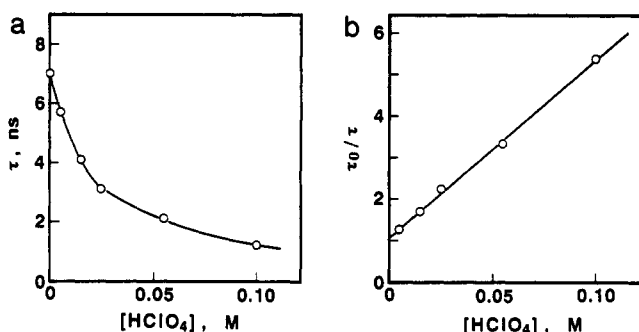


**Figure 3.** (a) Dependence of the fluorescence lifetime  $\tau$  of  $^1\text{AcrH}_2^*$  on  $[\text{HClO}_4]$  for the fluorescence quenching by  $\text{HClO}_4$  in MeCN containing  $\text{H}_2\text{O}$  (0.50 M) at 298 K. (b) Plot of  $\tau_0/\tau$  vs  $[\text{HClO}_4]$ .

shown in Figure 3a. From the slope of the Stern-Volmer plot in Figure 3b is obtained the rate constant of the protonation ( $k_H$ ) as  $6.1 \times 10^9 \text{ M}^{-1} \text{ s}^{-1}$ .

**Fluorescence Quenching by  $\text{R}_2\text{SOH}^+$ .** The fluorescence of  $\text{AcrH}_2$  is further quenched by addition of  $\text{R}_2\text{SO}$  in the presence of  $\text{HClO}_4$  in MeCN containing  $\text{H}_2\text{O}$  (0.50 M). In the absence of  $\text{HClO}_4$ , however, no fluorescence quenching has occurred by  $\text{R}_2\text{SO}$ . The ratio of the fluorescence intensities in the absence and presence of  $\text{Me}_2\text{SO}$  ( $I_0/I$ ) is plotted against the  $\text{Me}_2\text{SO}$  concentration at various concentrations of  $\text{HClO}_4$  as shown in Figure 4, where the  $I_0/I$  values increase with an increase in  $[\text{Me}_2\text{SO}]$  to reach a constant value. The saturated  $I_0/I$  values increase with an increase in  $[\text{HClO}_4]$ . Thus, the fluorescence quenching may occur by the protonated species, i.e.,  $\text{Me}_2\text{SOH}^+$ , the concentration of which varies depending on  $[\text{HClO}_4]$  according to the protonation equilibrium in eq 4.

The fluorescence quenching of  $\text{AcrH}_2$  by  $\text{R}_2\text{SOH}^+$  may occur by electron transfer from  $^1\text{AcrH}_2^*$  to  $\text{R}_2\text{SOH}^+$  as indicated by the energy diagram in Scheme I, where the energies required for electron transfer from  $\text{AcrH}_2$  and  $^1\text{AcrH}_2^*$  to  $\text{Me}_2\text{SO}$  and  $\text{Me}_2\text{SOH}^+$  (shown in parentheses) are compared. The  $\Delta H_f$  values are estimated as the calculated difference in the  $\Delta H_f$  (heat of formation) values by using the PM3 semiempirical molecular orbital method (see Experimental Section).<sup>17-20</sup> Although the reliability for the calculated  $\Delta H_f$  values which do not include the solvation energies precludes the quantitative comparison, the solvation energies in the charge shift reaction such that the total charge is unchanged ( $^1\text{AcrH}_2^* + \text{Me}_2\text{SOH}^+ \rightarrow \text{AcrH}_2^{2+} + \text{Me}_2\text{SOH}^*$ ) may be largely canceled out. Thus, the large exothermicity for the electron transfer from the singlet excited state ( $^1\text{AcrH}_2^*$ )<sup>25</sup> to the protonated species,  $\text{Me}_2\text{SOH}^+$  ( $-64.8 \text{ kcal mol}^{-1}$ ), as compared to the endothermic electron transfer from the ground state ( $\text{AcrH}_2$ ) to  $\text{Me}_2\text{SOH}^+$  ( $+16.6 \text{ kcal mol}^{-1}$ )

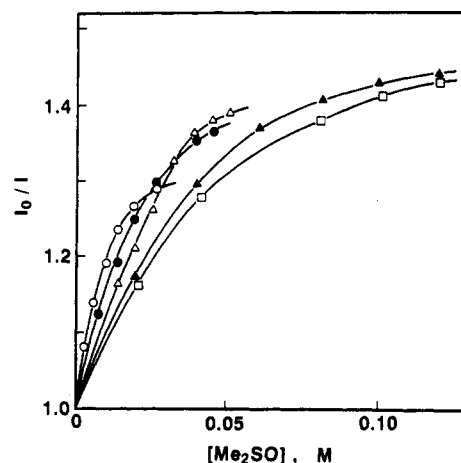


**Figure 4.** Stern-Volmer plots ( $I_0/I$  vs  $[\text{Me}_2\text{SO}]$ ) for the fluorescence quenching of  $^1\text{AcrH}_2^*$  by  $\text{Me}_2\text{SO}$  and  $\text{HClO}_4$  in MeCN containing  $\text{H}_2\text{O}$  (0.50 M) at 298 K.  $[\text{HClO}_4] = 1.4 \times 10^{-2}$  M (O),  $2.7 \times 10^{-2}$  M (●),  $4.0 \times 10^{-2}$  M ( $\Delta$ ),  $5.7 \times 10^{-2}$  M ( $\blacktriangle$ ), and  $8.4 \times 10^{-2}$  M ( $\square$ ).

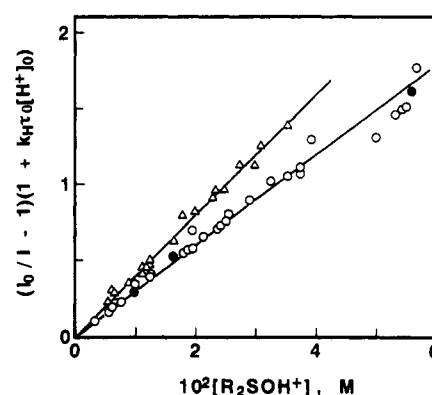
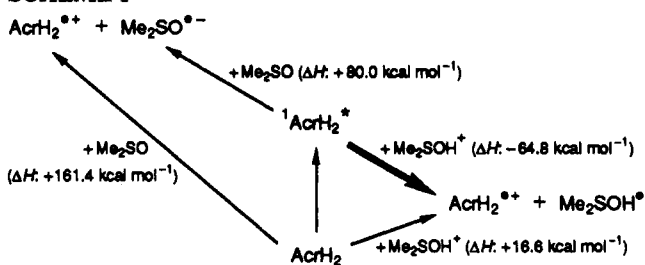


**Figure 5.** Plots of  $(I_0/I - 1)(1 + k_H\tau_0[\text{HClO}_4])$  vs  $[\text{R}_2\text{SOH}^+]$  for the fluorescence quenching of  $\text{AcrH}_2$  by  $\text{R}_2\text{SO}$ ,  $\text{R} = \text{Me}$  (O) and  $\text{Bu}$  ( $\Delta$ ) in the presence of  $\text{HClO}_4$  in MeCN containing  $\text{H}_2\text{O}$  (0.50 M) at 298 K. The values of  $\tau_0/\tau$  (●) are also plotted according to eq 7, where  $I_0/I$  is replaced by  $\tau_0/\tau$ .

#### SCHEME I



and that from  $\text{AcrH}_2$  and  $^1\text{AcrH}_2^*$  to  $\text{Me}_2\text{SO}$  ( $+161.4$  and  $+80.0 \text{ kcal mol}^{-1}$ , respectively), is unmistakable. In such a case the significant enhancement of the electron acceptor ability by the protonation of  $\text{Me}_2\text{SO}$  results in the efficient fluorescence quenching via exothermic electron transfer from the singlet excited state ( $^1\text{AcrH}_2^*$ ) to  $\text{Me}_2\text{SOH}^+$  (eq 6). In the presence of both

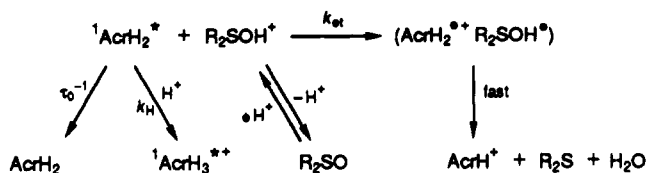


$\text{HClO}_4$  and  $\text{Me}_2\text{SO}$ , the fluorescence of  $\text{AcrH}_2$  is quenched by  $\text{H}^+$  (eq 5) as well as  $\text{Me}_2\text{SOH}^+$  (Scheme I). Then, the dependence of  $I_0/I$  on  $[\text{H}^+]$  and  $[\text{Me}_2\text{SOH}^+]$  is derived as given by eq 7, where  $\tau_0$  is the fluorescence lifetime of  $^1\text{AcrH}_2^*$  in the absence

$$(I_0/I - 1)(1 + k_H\tau_0[\text{H}^+]) = (k_{et} - k_H)\tau_0[\text{Me}_2\text{SOH}^+] \quad (7)$$

of  $\text{HClO}_4$  and  $\text{Me}_2\text{SO}$ . The data in the curved Stern-Volmer

## SCHEME II



plots in Figure 4 are plotted by using the relation in eq 7 as shown in Figure 5, where the  $[\text{Me}_2\text{SOH}^+]$  and  $[\text{H}^+]$  values in eq 7 are obtained from the  $K$  value ( $8.0 \times 10^2 \text{ M}^{-1}$ ) in eq 4 by using eqs 8 and 9 respectively). The fluorescence lifetime measurements

$$\begin{aligned}
 [\text{Me}_2\text{SOH}^+] &= ([\text{Me}_2\text{SO}]_0 + [\text{H}^+]_0 + K^{-1})/2 - \\
 &\{([\text{Me}_2\text{SO}]_0 + [\text{H}^+]_0 + K^{-1})^2 - 4[\text{Me}_2\text{SO}]_0[\text{H}^+]_0\}^{1/2}/2 \quad (8)
 \end{aligned}$$

$$[\text{H}^+] = [\text{H}^+]_0 - [\text{Me}_2\text{SOH}^+] \quad (9)$$

in the presence of  $\text{HClO}_4$  and  $\text{Me}_2\text{SO}$  should give essentially the same dependence on  $[\text{H}^+]$  and  $[\text{Me}_2\text{SOH}^+]$  as eq 7, provided that the fluorescence quenching by  $\text{Me}_2\text{SOH}^+$  is a dynamic process (eq 6). In fact, the dependence of  $\tau_0/\tau$  values on  $[\text{H}^+]$  and  $[\text{Me}_2\text{SO}]$  agrees well with eq 7 in which  $I_0/I$  is replaced by  $\tau_0/\tau$  as also shown in Figure 5. From the slopes of the linear plots in Figure 5 are obtained the  $k_{et}$  value of electron transfer from  ${}^1\text{AcrH}_2^*$  to  $\text{Me}_2\text{SOH}^+$  and  $\text{Bu}_2\text{SOH}^+$  as  $1.0 \times 10^{10}$  and  $1.1 \times 10^{10} \text{ M}^{-1} \text{ s}^{-1}$ , respectively. Thus, electron transfer from  ${}^1\text{AcrH}_2^*$  to  $\text{Me}_2\text{SOH}^+$  and  $\text{Bu}_2\text{SOH}^+$  occurs efficiently with the rates being close to diffusion-controlled.

**Mechanism of Acid-Catalyzed Photoreduction of  $\text{R}_2\text{SO}$  by  $\text{AcrH}_2$ .** Based on the above results, the reaction mechanism of the acid-catalyzed photoreduction of  $\text{R}_2\text{SO}$  by  $\text{AcrH}_2$  may be summarized as shown in Scheme II. The protonation of  $\text{R}_2\text{SO}$  enhances the electron acceptor ability, resulting in efficient electron transfer from  ${}^1\text{AcrH}_2^*$  to  $\text{R}_2\text{SOH}^+$  ( $k_{et}$ ) to give the radical pair ( $\text{AcrH}_2^{*+} \text{R}_2\text{SOH}^*$ ). At the same time, however, the quenching of  ${}^1\text{AcrH}_2^*$  by  $\text{H}^+$  ( $k_H$ ) reduces the lifetime of  ${}^1\text{AcrH}_2^*$ . In order to know the feasible subsequent reaction process, the  $\Delta H_f$  values of  $\text{AcrH}_2^{*+}$ ,  $\text{AcrH}^+$ ,  $\text{Me}_2\text{SOH}^*$ ,  $\text{Me}_2\text{SH}(\text{OH})$ ,  $\text{Me}_2\text{S}$ , and  $\text{H}_2\text{O}$  are calculated by using the PM3 method (see Experimental Section).<sup>17-20</sup> The calculated difference in the  $\Delta H_f$  values for the hydrogen transfer from  $\text{AcrH}_2^{*+}$  to  $\text{Me}_2\text{SOH}^*$  to yield  $\text{AcrH}^+$  and  $\text{Me}_2\text{SH}(\text{OH})$  is largely positive,  $+27.4 \text{ kcal mol}^{-1}$ , while that for the hydrogen transfer accompanied by the dehydration of  $\text{Me}_2\text{SH}(\text{OH})$  to yield  $\text{AcrH}^+$ ,  $\text{Me}_2\text{S}$ , and  $\text{H}_2\text{O}$  is largely negative,  $-26.3 \text{ kcal mol}^{-1}$ . Thus, the hydrogen transfer from  $\text{AcrH}_2^{*+}$  to  $\text{Me}_2\text{SOH}^*$  may be accompanied by the concomitant dehydration to yield the final product,  $\text{AcrH}^+$ ,  $\text{R}_2\text{S}$ , and  $\text{H}_2\text{O}$  (Scheme II). The hydrogen transfer process may not be the rate-determining step, since no primary kinetic isotope effects have been observed in the overall quantum yields (Figure 2).<sup>25</sup>

By applying the steady-state approximation to the reactive species  ${}^1\text{AcrH}_2^*$  and ( $\text{AcrH}_2^{*+} \text{R}_2\text{SOH}^*$ ) in Scheme II, the overall quantum yield can be derived as given by eq 10. Since the  $k_{et}\tau_0$

$$\Phi = k_{et}\tau_0K[\text{R}_2\text{SO}][\text{H}^+]/(1 + k_H\tau_0[\text{H}^+] + k_{et}\tau_0K[\text{R}_2\text{SO}][\text{H}^+]) \quad (10)$$

and  $k_H\tau_0$  values are already determined by the fluorescence quenching by  $\text{H}^+$  and  $\text{Me}_2\text{SOH}^+$  (Figure 3 and Figure 5), the dependence of the quantum yield on  $[\text{H}^+]$  and  $[\text{Me}_2\text{SOH}^+]$  (the concentrations are obtained from the protonation equilibrium constant  $K$  by using eqs 8 and 9) can be calculated by using eq 10. The calculated dependence of the quantum yield  $\Phi$  on  $[\text{HClO}_4]$  at a fixed concentration of  $\text{Me}_2\text{SO}$  ( $3.4 \times 10^{-3} \text{ M}$ ) shown by the solid line in Figure 2 agrees well with the

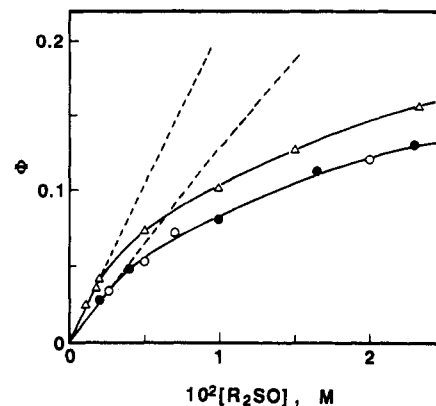
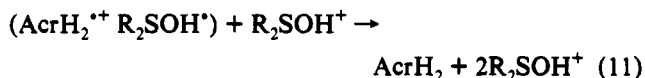


**Figure 6.** Dependence of  $\Phi$  on  $[\text{R}_2\text{SO}]$  for the photoreduction of  $\text{R}_2\text{SO}$  [ $\text{R} = \text{Me}$  ( $\circ$ ) and  $\text{Bu}$  ( $\Delta$ ) by  $\text{AcrH}_2$  ( $\circ$ ,  $\Delta$ ) and  $\text{AcrD}_2$  ( $\bullet$ )] in the presence of  $\text{HClO}_4$  (0.10 M) and  $\text{H}_2\text{O}$  (0.50 M) in  $\text{MeCN}$  at 298 K. The broken lines are drawn with the rate constants ( $k_{et}$  and  $k_H$ ), the fluorescence lifetime ( $\tau_0$ ), and the protonation equilibrium constant ( $K$ ) by using eq 10.

experimental results. Such agreement strongly indicates the validity of the reaction mechanism in Scheme II.

The dependence of the quantum yield on  $[\text{R}_2\text{SO}]$  for the photoreduction of  $\text{R}_2\text{SO}$  by  $\text{AcrH}_2$  and  $\text{AcrD}_2$  at a fixed concentration of  $\text{HClO}_4$  (0.10 M) was also examined as shown in Figure 6.<sup>27</sup> It is confirmed that no appreciable primary kinetic isotope effect is observed at different concentrations of  $\text{Me}_2\text{SO}$ . The broken lines in Figure 6 show the calculated dependence based on eq 10. At low concentrations of  $\text{Me}_2\text{SO}$  and  $\text{Bu}_2\text{SO}$  the calculated  $\Phi$  values agree well with the experimental values. With an increase in  $[\text{R}_2\text{SO}]$ , however, the experimental values become smaller than the calculated values based on eq 10. Such a retarding effect of  $\text{R}_2\text{SO}$  in the presence of  $\text{HClO}_4$  may be caused by the electron exchange between  $\text{R}_2\text{SOH}^*$  and  $\text{R}_2\text{SOH}^+$ , which interrupts the hydrogen transfer leading to the final products, resulting in the back electron transfer from  $\text{R}_2\text{SOH}^*$  to  $\text{AcrH}_2^{*+}$  to regenerate the reactant pair (eq 11).<sup>28</sup>



In conclusion, the catalytic function of acid in the photoreduction of  $\text{R}_2\text{SO}$  by  $\text{AcrH}_2$  is attributed to the protonation of the ground-state substrate, which enhances the electron transfer from the singlet excited state  ${}^1\text{AcrH}_2^*$  significantly. In order to achieve the high efficiency of the acid-catalyzed photoreduction, the concentration of acid should be optimized, since the acid can also retard the reaction through the quenching of  ${}^1\text{AcrH}_2^*$  (Scheme II) and also by facilitating the back electron transfer (eq 11).

**Acknowledgment.** This work was supported in part by a grant-in-aid for scientific research from the Ministry of Education, Science and Culture, Japan.

## References and Notes

- (1) Fukuzumi, S.; Tanaka, T. In *Photoinduced Electron Transfer*; Fox, M. A., Chanon, M., Eds.; Elsevier: Amsterdam, 1988; Part C, Chapter 10, p 636, and references cited therein.
- (2) (a) Fujii, M.; Nakamura, K.; Mekata, H.; Oka, S.; Ohno, A. *Bull. Chem. Soc. Jpn.* **1988**, *61*, 495. (b) Fukuzumi, S.; Ishikawa, M.; Tanaka, T. *J. Chem. Soc., Perkin Trans. 2* **1989**, 1037. (c) Ishikawa, M.; Fukuzumi, S. *J. Am. Chem. Soc.* **1990**, *112*, 8864. (d) Deng, G.; Xu, H.-J.; Chen, D.-W. *J. Chem. Soc., Perkin Trans. 2* **1990**, 1133. (e) Ohkubo, K.; Yamashita, K.; Ishida, H.; Haramaki, H.; Sakamoto, Y. *J. Chem. Soc., Perkin Trans. 2* **1991**, 1833.
- (3) Fukuzumi, S. In *Advances in Electron Transfer Chemistry*; Mariano, P. S. Ed.; JAI Press: Greenwich, 1992; Vol. 2, p 65.
- (4) (a) van Eikeren, P.; Grier, D. L. *J. Am. Chem. Soc.* **1976**, *98*, 4655. (b) Shinkai, S.; Hamada, H.; Kusano, Y.; Manabe, O. *J. Chem. Soc., Perkin Trans. 2* **1979**, 699. (c) Shinkai, S.; Hamada, H.; Manabe, O. *Tetrahedron Lett.* **1979**, 1397. (d) Ohno, A.; Ishikawa, Y.; Ushida, S.; Oka, S. *Tetrahedron*

- Lett.* **1982**, *23*, 3185. (e) Fukuzumi, S.; Ishikawa, M.; Tanaka, T. *J. Chem. Soc., Chem. Commun.* **1985**, 1069. (f) Awano, A.; Tagaki, W. *Bull. Chem. Soc. Jpn.* **1986**, *59*, 3117. (g) Singh, S.; Gill, S.; Sharma, V. K.; Nagrath, S. *J. Chem. Soc., Perkin Trans. 1* **1986**, 1273. (h) Fukuzumi, S.; Ishikawa, M.; Tanaka, T. *Tetrahedron* **1986**, *42*, 1021. (i) Fukuzumi, S.; Chiba, M.; Tanaka, T. *Chem. Lett.* **1989**, 31. (j) Fukuzumi, S.; Mochizuki, S.; Tanaka, T. *J. Am. Chem. Soc.* **1989**, *111*, 1497. (k) Fukuzumi, S.; Ishikawa, M.; Tanaka, T. *J. Chem. Soc., Perkin Trans. 2* **1989**, 1811. (l) Fujii, M.; Aida, T.; Yoshihara, M.; Ohno, A. *Bull. Chem. Soc. Jpn.* **1989**, *62*, 3845. (m) Fukuzumi, S.; Mochizuki, S.; Tanaka, T. *Inorg. Chem.* **1990**, *29*, 653. (n) Ishikawa, M.; Fukuzumi, S. *J. Chem. Soc., Chem. Commun.* **1990**, 1353.
- (5) (a) de Bont, J. A. M.; van Dijken, J. P.; Harder, W. *J. Gen. Microbiol.* **1981**, *127*, 315. (b) Yen, H.-C.; Marrs, B. *Arch. Biochem. Biophys.* **1977**, *181*, 411. (c) Zinder, S. H.; Brock, T. D. *J. Gen. Microbiol.* **1978**, *105*, 335.
- (6) (a) Wubbels, G. G. *Acc. Chem. Res.* **1983**, *16*, 285. (b) Albini, A. *J. Chem. Educ.* **1986**, *63*, 383. (c) Wan, P.; Yates, K. *Rev. Chem. Intermed.* **1984**, *5*, 157.
- (7) (a) McEwen, J.; Yates, K. *J. Am. Chem. Soc.* **1987**, *109*, 5800. (b) Wubbels, G. G.; Susens, D. P.; Coughlin, E. B. *J. Am. Chem. Soc.* **1988**, *110*, 2538. (c) Wubbels, G. G.; Snyder, E. J.; Coughlin, E. B. *J. Am. Chem. Soc.* **1988**, *110*, 2543. (d) Chow, Y. L.; Buono-Core, G. E.; Zhang, Y.-H.; Liu, X.-Y. *J. Chem. Soc., Perkin Trans. 2* **1991**, 2041. (e) Renneke, R. F.; Kadkhodayan, M.; Pasquali, M.; Hill, C. L. *J. Am. Chem. Soc.* **1991**, *113*, 8357.
- (8) (a) Lewis, F. D.; Barancyk, S. V. *J. Am. Chem. Soc.* **1989**, *111*, 8653. (b) Lewis, F. D.; Quillen, S. L.; Hale, P. D.; Oxman, J. D. *J. Am. Chem. Soc.* **1988**, *110*, 1261. (c) Lewis, F. D.; Howard, D. K.; Oxman, J. D.; Uthagrove, A. L.; Quillen, S. L. *J. Am. Chem. Soc.* **1986**, *108*, 5964. (d) Lewis, F. D.; Howard, D. K.; Barancyk, S. V.; Oxman, J. D. *J. Am. Chem. Soc.* **1986**, *108*, 3016. (e) Lewis, F. D.; Oxman, J. D.; Gibson, L. L.; Hampsch, H. L.; Quillen, S. L. *J. Am. Chem. Soc.* **1986**, *108*, 3005.
- (9) (a) Fukuzumi, S.; Ishikawa, K.; Hironaka, K.; Tanaka, T. *J. Chem. Soc., Perkin Trans. 2* **1987**, 751. (b) Fukuzumi, S.; Tani, K.; Tanaka, T. *J. Chem. Soc., Chem. Commun.* **1989**, 816. (c) Fukuzumi, S.; Mochizuki, S.; Tanaka, T. *J. Phys. Chem.* **1990**, *94*, 722.
- (10) A preliminary report has appeared: Fukuzumi, S.; Tokuda, S. *Chem. Lett.* **1991**, 897.
- (11) (a) Oppenheimer, N. J. In *Pyridine Nucleotide Coenzymes*; Dolphin, D., Avramovic, O.; Poulson, R., Eds.; Wiley-Interscience: New York, 1987; Part A, p 323. (b) Skibo, E. B.; Bruice, T. C. *J. Am. Chem. Soc.* **1983**, *105*, 3316. (c) van Eikeren, P.; Grier, D. L.; Eliason, J. *J. Am. Chem. Soc.* **1979**, *101*, 7406.
- (12) Roberts, R. M. G.; Ostović, D.; Kreevoy, M. M. *Faraday Discuss. Chem. Soc.* **1982**, *74*, 257.
- (13) Fukuzumi, S.; Koumitsu, S.; Hironaka, K.; Tanaka, T. *J. Am. Chem. Soc.* **1987**, *109*, 305.
- (14) (a) Ostović, D.; Roberts, R. M. G.; Kreevoy, M. M. *J. Am. Chem. Soc.* **1983**, *105*, 7629. (b) Kreevoy, M. M.; Lee, I.-S. H. *J. Am. Chem. Soc.* **1984**, *106*, 2550.
- (15) Perrin, D. D.; Armarego, W. L. F.; Perrin, D. R. *Purification of Laboratory Chemicals*; Pergamon Press: England, 1966.
- (16) (a) Hatchard, C. G.; Parker, C. A. *Proc. R. Soc. London, Ser. A* **1956**, *235*, 518. (b) Calvert, J. C.; Pitts, J. N. *Photochemistry*; Wiley: New York, 1966; p 783.
- (17) Stewart, J. J. P. *J. Comput. Chem.* **1989**, *10*, 209, 221.
- (18) (a) Dewar, M. J. S.; Thiel, W. *J. Am. Chem. Soc.* **1977**, *99*, 4899. (b) Dewar, M. J. S.; Thiel, W. *J. Am. Chem. Soc.* **1977**, *99*, 4907.
- (19) Toyoda, J. *JCPE News Lett.* **1990**, *2*, 37.
- (20) Clark, T. *A Handbook of Computational Chemistry*; Wiley: New York, 1985; p 97.
- (21) Fukuzumi, S.; Chiba, M.; Ishikawa, M.; Ishikawa, K.; Tanaka, T. *J. Chem. Soc., Perkin Trans. 2* **1989**, 1417.
- (22) (a) Bordwell, F. G. *Acc. Chem. Res.* **1988**, *21*, 456. (b) Bausch, M. J.; Guadalupe-Fasano, C.; Koohang, A. *J. Phys. Chem.* **1991**, *95*, 3420.
- (23) In the absence of added H<sub>2</sub>O, the protonation equilibrium constant is too large to be determined accurately.
- (24) Fukuzumi, S.; Kuroda, S.; Goto, T.; Ishikawa, K.; Tanaka, T. *J. Chem. Soc., Perkin Trans. 2* **1989**, 1047.
- (25) The calculated excitation energy (81.4 kcal mol<sup>-1</sup> = 3.53 eV) is compatible with the zero-zero excitation energy obtained from the frequencies of the absorption and emission maxima (3.90 eV).<sup>1</sup>
- (26) No kinetic deuterium isotope effects in electron transfer reactions are expected except for those involving substantial inner-sphere reorganization, in which a small deuterium isotope effect (1.3) has been reported; Guarr, T.; Buhks, E.; McLendon, G. *J. Am. Chem. Soc.* **1983**, *105*, 3763.
- (27) The increase of H<sub>2</sub>O concentration from 0.50 to 2.0 M resulted in no appreciable change in the results in Figure 6.
- (28) The retarding effect of R<sub>2</sub>SO in the presence of HClO<sub>4</sub> might be ascribed to specific solvation effects such as formation of clusters, (R<sub>2</sub>SO)<sub>n</sub>H<sup>+</sup>, which would be expected to be less reactive than R<sub>2</sub>SOH<sup>+</sup>. However, such solvation effects are not apparent in the spectral change with [HClO<sub>4</sub>] in Figure 1.